

# The Annular Flow, Electrothermal Plug Ramjet

B. D. Shaw,\* C. E. Mitchell,† and P. J. Wilbur‡  
*Colorado State University, Fort Collins, Colorado*

The annular flow, electrothermal plug ramjet is examined as a possible means of achieving rapid projectile acceleration for applications such as direct space payload launches. Electrothermal plug ramjet performance is examined for cases when hydrogen propellant is treated 1) as a perfect gas and 2) as a gas that can dissociate and ionize and then recombine at finite rates in the nozzle. Performance results for these cases are compared to the performance of a conventional ramjet operating with a perfect gas hydrogen propellant. Models describing electrothermal plug ramjet and conventional ramjet operation are presented and it is shown that, for a given flight velocity, there is an optimum rate of heat addition per unit mass of propellant. Propellant dissociation and ionization losses are found to be small and the nozzle flow is shown to be near chemical equilibrium rather than in a chemically frozen state. Diffuser shock losses are found not to degrade performance to unacceptably low levels. Fluid particle residence times are found to be small compared with those required for significant flowfield changes and it is argued that assuming quasisteady flow does not introduce significant errors. Thermal efficiencies over selected launch cycles are between 30 and 40% and pressure, temperature, and power requirements are demonstrated to be reasonable.

## Nomenclature

$A$	= flow area, $m^2$
$B, C, D, E, K$	= constants used in Eqs. (8-11)
$d$	= diameter, $m$
$F$	= thrust, $N$
$g$	= acceleration due to gravity, $9.8 \text{ m/s}^2$
$M$	= Mach number
$P$	= static pressure, $Pa$
$P_T$	= stagnation pressure, $Pa$
$\dot{Q}$	= heat addition rate, $W$
$q$	= heat addition per unit mass, $J/kg$
$T$	= static temperature, $K$
$T_T$	= stagnation temperature, $K$
$V$	= velocity, $m/s$
$\delta$	= conical diffuser half-angle, $deg$
$\gamma$	= ratio of specific heats
$\rho$	= density, $kg/m^3$
$\sigma$	= acceleration, $g$

(A numerical subscript on a variable corresponds to a fluid state defined in Figs. 1a and/or 1b.)

## Introduction

**D**IRECT-launch systems are currently being considered for space resupply and disposal missions where high accelerations can be tolerated. Payloads delivered into space with these systems would be accelerated to very high velocities (on the order of  $10^4 \text{ m/s}$ ) close to the Earth's surface and they would then be slowed somewhat to the desired final energy during passage through the Earth's atmosphere. One such system that has been proposed recently for such missions is the electrothermal ramjet.<sup>1</sup> This system appears to be capable of achieving the high acceleration levels needed to assure launch

tracks that are of a reasonable length primarily because it does not accelerate either the propellant or the powerplant required to effect its operation.

Conceptually, the electrothermal ramjet involves a long tube filled with gaseous propellant through which a ramjet engine is accelerated to a specified terminal velocity. Typically, the ramjet would be operated at constant thrust using hydrogen propellant heated by either electromagnetic radiation or electrical currents as it passes through the ramjet. Energy would either be beamed or conducted to the ramjet heat addition zone from the tube walls as the ramjet passed down the launch tube. Because a ramjet requires a substantial initial velocity before it can begin to produce thrust, it is anticipated that the ramjet would be accelerated to this velocity by a device such as a light gas gun. Preliminary analysis<sup>1,2</sup> has suggested that a particular ramjet configuration referred to as the annular flow plug ramjet is well suited to this application and that such a device should exhibit good performance.

The purpose of this paper is to 1) compare the performance of the annular flow plug ramjet to the more familiar conventional ramjet, 2) demonstrate that losses due to diffuser shocks, while significant, do not degrade performance to an unacceptably low level, and 3) demonstrate that dissociation and ionization losses in the hydrogen propellant are small and that the nozzle flow in these devices is typically near thermodynamic equilibrium.

The analysis on which this paper is based involves extensive modeling of both the fluid mechanics of the problem and hydrogen properties and must be executed on a high-speed digital computer. However, the physical principles governing operation of the device can be illustrated rather simply through the basic relationships describing ramjet performance. These will be presented and data obtained from the more complete analysis will be interpreted in the light of these relationships.

## Theoretical Models

The general concept of a conventional ramjet is shown in Fig. 1a. The reference frame is chosen to be moving with the ramjet, so the propellant is shown moving toward the inlet with a velocity  $V_1$ . The Mach number associated with the incoming flow is designated  $M_1$ . After the ramjet has been accelerated to a high enough initial velocity, an oblique shock

Received July 30, 1984; revision received April 26, 1985. Copyright © American Institute of Aeronautics and Astronautics, Inc., 1985. All rights reserved.

\*Research Assistant, Department of Mechanical Engineering.

†Professor, Department of Mechanical Engineering.

‡Professor, Department of Mechanical Engineering. Member AIAA.

will be attached to the conical tip of the center body that serves as a diffuser. Downstream of the diffuser tip, a series of shocks reflected between the center and outer bodies will occur. They will terminate in a normal shock that will slow the flow to subsonic conditions. A review of the hypersonic wind tunnel literature<sup>3</sup> has suggested that normal shock recovery can be expected after the initial conical shock, so it is assumed that the flow passes through an initial conical shock to state 2 and then passes through a single normal shock to state 3. One-dimensional values obtained by averaging over the axisymmetric conical flowfield variables computed at the exit to the conical flowfield in region 2 are used as input for the normal shock relations. Across the normal shock, equations describing mass continuity, the first law of thermodynamics, conservation of momentum, and the second law of thermodynamics are satisfied. Immediately downstream of the normal shock, it is sufficient so that the flow will pass through the minimum area encountered at the diffuser throat. After the normal shock, the flow enters the subsonic heat addition region at 4 and heat is assumed to be deposited into the flow between states 4 and 5. In the heat addition region, the first and second laws of thermodynamics are satisfied, along with mass continuity and the momentum equation. After leaving the heat addition region at 5, the flow passes through a converging-diverging channel where it is accelerated first to the sonic condition at state 6 and then on to supersonic conditions at the nozzle exit 7.

With this convention ramjet (Fig. 1a), the static inlet and outlet pressures are equal because the freestream conditions are communicated outside of the moving outer body. In order to satisfy this condition while assuming no shocks in the nozzle, one finds the nozzle exit area ( $A_7$ ) must be larger than the free-flow diffuser inlet area ( $A_1$ ). It is hoped that by comparing this more familiar ramjet to the new one being proposed that the concept and performance of the plug ramjet can be better understood.

The annular flow plug ramjet is shown in Fig. 1b. It appears similar to the conventional ramjet at first glance, but is different in the following ways:

1) The plug ramjet moves down the tube as the center body of the conventional ramjet does, but in the former case the outer body is the launch tube (which is stationary). Because the launch tube diameter is essentially constant along its length, the fluid mechanics and thermodynamics of the problem can again be considered from the frame of reference of the ramjet as though this tube were not moving.

2) The inlet and outlet areas associated with flow through the plug ramjet ( $A_7$ ) must be equal, again because the launch

tube diameter does not vary significantly along its length.

3) The inlet and outlet pressures  $P_1$  and  $P_7$  are not equal because the upstream and downstream regions are not connected through an exterior path. In fact, the outlet pressure  $P_7$  will be greater than the inlet pressure  $P_1$  and, therefore, this pressure difference will produce some component of the thrust exerted on the plug.

One can see that the fluid mechanics of both problems in Figs. 1a and 1b are described by the same basic equations. The only difference in the two cases is the difference in the boundary conditions applied to the flow.

In this analysis, the fluid flow is always assumed to be in a quasisteady state and the conical diffuser nose is always assumed to operate at zero angle of attack. The propellant considered is hydrogen. For purposes of comparison and completeness, perfect-gas analyses and analyses that consider dissociation and ionization along with internal molecular and atomic modes of energy storage are conducted. Results from statistical mechanics are used to compute equilibrium thermodynamic properties and shifting chemical composition is allowed to occur in the analyses, which include dissociation and ionization. Where they are deemed potentially important, nonequilibrium processes are evaluated by considering finite rate reactions. The ideal-gas equation of state is assumed to be valid at all times. Because the essence of the phenomena occurring in these devices is described by the perfect-gas model and because the models that consider dissociation and ionization are complex and difficult to describe briefly, only the perfect-gas model will be presented here. It is simply stated that the complex model requires numerical application of the momentum, mass continuity, and energy equations along with com-

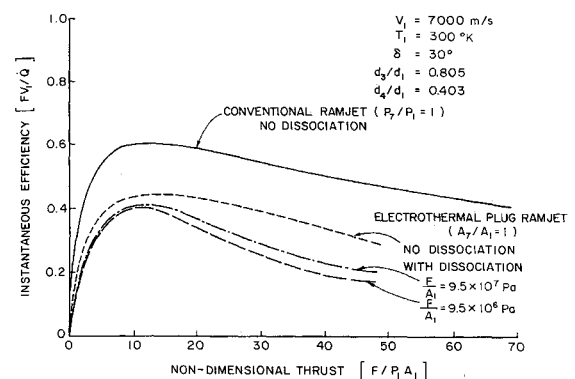


Fig. 2 Instantaneous efficiency profiles.

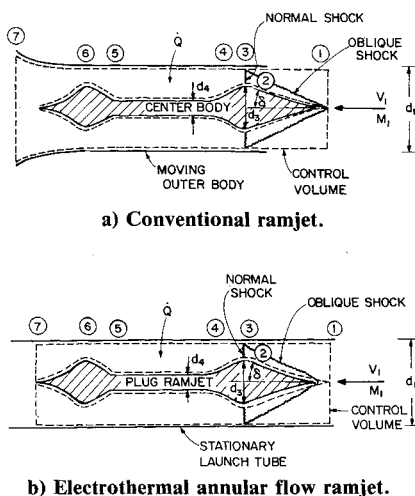


Fig. 1 Ramjet configurations.

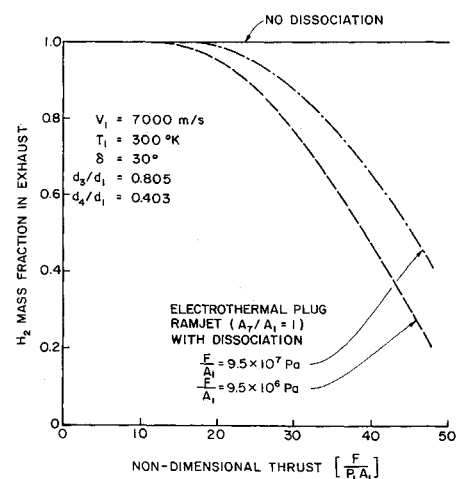


Fig. 3 Mass fraction of  $H_2$  in exhaust.

plex hydrogen composition models between each pair of state points shown in Fig. 1.

### Perfect-Gas Models

Consider now that either ramjet in Fig. 1 is being accelerated at a constant thrust  $F$  and that heat is being added at a rate  $\dot{Q}$  to achieve this level of thrust. In general,  $\dot{Q}$  will vary with the velocity of the ramjet and will be different for the conventional and plug designs. By assuming that the propellant flowing through the control volumes shown in Fig. 1 behaves as a perfect gas, the momentum equation applied across the control volumes of Fig. 1 can be put in the following form:

$$\frac{F}{P_1 A_1} = \frac{A_7}{A_1} \frac{P_{T_7}}{P_{T_1}} \left[ \frac{1 + [(\gamma - 1)/2] M_1^2}{1 + [(\gamma - 1)/2] M_7^2} \right]^{\gamma/(\gamma - 1)} \times (\gamma M_7^2 + 1) - (\gamma M_1^2 + 1) \quad (1)$$

In this equation, the entrance and exit conditions are, respectively, Mach number  $M_1$ ,  $M_7$ ; area  $A_1$ ,  $A_7$ ; and stagnation pressure  $P_{T_1}$ ,  $P_{T_7}$ .  $\gamma$  is the ratio of specific heats and  $P_1$  the entrance static pressure. The left-hand side of this equation represents a nondimensionalized thrust. The stagnation pressure ratio appearing in Eq. (1) can be written

$$\frac{P_{T_7}}{P_{T_1}} = \frac{P_{T_4}}{P_{T_1}} \frac{P_{T_5}}{P_{T_4}} \frac{P_{T_7}}{P_{T_5}} \quad (2)$$

where  $P_{T_4}/P_{T_1}$ , the stagnation pressure ratio across the diffuser, is less than unity because of diffuser losses. The heat addition region stagnation pressure ratio  $P_{T_5}/P_{T_4}$  is also less than unity because of heat addition-induced stagnation pressure losses. Because the nozzle is assumed to be isentropic, the ratio  $P_{T_7}/P_{T_5}$  is unity.

When the first law of thermodynamics is applied to a perfect-gas working fluid, the following expression for the instantaneous ramjet efficiency (power into ramjet mass acceleration divided by input thermal power) is obtained:

$$\frac{FV_1}{\dot{Q}} = \frac{F}{P_1 A_1} \frac{\gamma - 1}{\gamma} \left[ \left( 1 + \frac{\gamma - 1}{2} M_1^2 \right) \left( \frac{T_{T_7}}{T_{T_1}} - 1 \right) \right]^{-1} \quad (3)$$

To apply these equations to the analysis of either ramjet, it is necessary to specify the inlet Mach number  $M_1$  and the diffuser geometry so that the diffuser stagnation pressure ratio  $P_{T_4}/P_{T_1}$  can be computed. For a given conical diffuser half-angle  $\delta$ , annular diffuser shoulder diameter  $d_3$ , and heat addition centerbody diameter  $d_4$ , the inlet free-flow diameter  $d_1$  is specified by placing the intersection of the conical shock and the outer body or tube wall at the annular diffuser shoulder. Specifying these parameters serves to fix the flow conditions up to state 4, where subsonic conditions are always specified. Because the propellant is assumed to behave as a perfect gas, the Taylor-Maccoll method<sup>4</sup> for analyzing conical flowfields is utilized to describe the flowfield downstream of the conical shock. The axisymmetric conical flowfield variables at the entrance to the normal shock are next conservation to one-dimensional form by using a mass-averaging procedure that satisfies the equations of mass continuity and energy conservation. These one-dimensional values of the variables are then used as input to the normal shock relations so the stagnation pressure ratio  $P_{T_4}/P_{T_1}$  and the flow conditions downstream of the normal shock 3 can be utilized to specify the conditions at the entrance to the heat addition region 4. By knowing  $M_4$  and specifying  $M_5$ , the heat addition stagnation pressure ratio  $P_{T_5}/P_{T_4}$  is fixed, as is the stagnation temperature ratio

$(T_{T_5}/T_{T_4} = T_{T_7}/T_{T_1})$ . To analyze ramjet operation then, either the exit/inlet area ratio  $A_7/A_1$  or the exit/inlet static pressure ratio  $P_7/P_1$  may be specified to fix  $M_7$ . For the conventional ramjet the pressure ratio  $P_7/P_1$  is set to unity and for the electrothermal ramjet the area ratio  $A_7/A_1$  is set to unity. It is noteworthy that the parameters  $A_7/A_1$ ,  $P_7/P_1$ , and  $M_7$  are not completely independent. Specifying one parameter dictates values for the others.

Dictating the exit/inlet conditions for a ramjet control volume allows the calculation of other parameters, such as the exit/inlet velocity and temperature ratios, and the fractions of the total thrust provided by 1) the difference in the pressure area product between the entrance and exit flowfields and 2) the momentum change in the propellant. The mathematical relationships utilized to compute these ratios and fractions are not shown here, but the graphical results are illustrated in the Results section of this paper for specific operating conditions.

To further illustrate the performance of the ramjets operating with a perfect-gas propellant, it is instructive to express the first law of thermodynamics in the form

$$\frac{V_7}{V_1} = \left( \frac{T_{T_7}}{T_{T_1}} \right)^{1/2} \left\{ \frac{2}{M_1^2 (\gamma - 1)} \left[ 1 - \left( \frac{P_{T_7}}{P_{T_1}} \frac{P_1}{P_7} \right)^{(1-\gamma)/\gamma} \right] + 1 \right\}^{1/2} \quad (4)$$

and the momentum equation in the form

$$\frac{F}{\dot{m} V_1} = \left( \frac{V_7}{V_1} - 1 \right) + \frac{1}{M_1^2 \gamma} \left[ \frac{T_{T_7}}{T_{T_1}} \times \left( \frac{P_{T_7}}{P_{T_1}} \frac{P_1}{P_7} \right)^{(1-\gamma)/\gamma} \frac{1}{(V_7/V_1)} - 1 \right] \quad (5)$$

Equation (5) can be multiplied by the quantity

$$\frac{V_1^2}{[\gamma/(\gamma - 1)] R T_{T_1} [(T_{T_7}/T_{T_1}) - 1]} \quad (6)$$

to obtain the form

$$\frac{FV_1}{\dot{Q}} = \frac{(\gamma - 1) M_1^2}{[1 + [(\gamma - 1)/2] M_1^2] [(T_{T_7}/T_{T_1}) - 1]} \left\{ \left( \frac{V_7}{V_1} - 1 \right) + \frac{1}{M_1^2 \gamma} \left[ \frac{T_{T_7}}{T_{T_1}} \left( \frac{P_{T_7}}{P_{T_1}} \frac{P_1}{P_7} \right)^{(1-\gamma)/\gamma} \frac{1}{(V_7/V_1)} - 1 \right] \right\} \quad (7)$$

For the conventional ramjet,  $P_7/P_1 = 1$ . The stagnation pressure ratio  $P_{T_7}/P_{T_1}$  is given by

$$\frac{P_{T_7}}{P_{T_1}} = \frac{P_{T_4}}{P_{T_1}} \frac{P_{T_5}}{P_{T_4}} \frac{P_{T_7}}{P_{T_5}}$$

where  $P_{T_4}/P_{T_1}$  is fixed by the inlet flow condition and the diffuser geometry and  $P_{T_7}/P_{T_5}$  is unity. The stagnation pressure ratio  $P_{T_5}/P_{T_4}$  is dictated by the rate of heat addition per unit mass to the propellant; for subsonic heat addition, this ratio does not vary appreciably. Examination of Eq. (4) shows that for fixed values of  $M_1$ ,  $\gamma$ ,  $P_{T_4}/P_{T_1}$ , and  $P_{T_7}/P_{T_5}$ , the effect of the variation of  $P_{T_5}/P_{T_4}$  on the expression in brackets

$$\left\{ \frac{2}{M_1^2 (\gamma - 1)} \left[ 1 - \left( \frac{P_{T_7}}{P_{T_1}} \frac{P_1}{P_7} \right)^{(1-\gamma)/\gamma} \right] + 1 \right\}^{1/2}$$

is small compared to the change in

$$(T_{T_7}/T_{T_1})^{1/2}$$

as the rate of heat addition per unit mass is varied. As a result, Eq. (4) can be written as

$$V_7/V_1 = K_1 (T_{T7}/T_{T1})^{1/2} \quad (8)$$

where  $K_1$  is approximately constant. The variation in  $K_1$  is typically of the order of 5% for the cases considered.

#### Dissociating Flow Model

It was anticipated that assuming the propellant behaves as a perfect gas would introduce errors into these analyses, because such effects as vibrational and electronic excitation, dissociation, and ionization of the propellant could play significant roles in the performance of a ramjet device. The annular flow electrothermal ramjet was also analyzed with these effects included. The validity of assuming either chemically frozen or equilibrium chemical composition in the supersonic nozzle expansion was also evaluated. In analyzing the flow in the diffuser for this dissociating flow case, it was assumed that the fluid in the conical flowfield between the normal shock and the oblique shock behaved as a perfect gas and thus that this portion of the model developed for the perfect-gas models could be applied. This assumption should not introduce too much error into this analysis, because the oblique shock angle should be shallow for high inlet velocities and small diffuser cone angles and the temperature rise in the conical flowfield should not be too large. Downstream of the normal shock, chemical relaxation and other nonperfect-gas modes of energy storage were allowed to occur in the propellant. The propellant was assumed to be in thermodynamic equilibrium downstream of the normal shock and up to the annular nozzle throat exit 6. Finite chemical reaction rates were evaluated in the supersonic nozzle expansion between states 6 and 7. Because a shifting chemical equilibrium was allowed, the closed-form equations for the thermodynamic properties could not be obtained. The method of analysis utilized for the model including shifting composition involved piece wise application of the momentum and energy equations between each state identified in Fig. 1 that is downstream of the normal shock.

In order to compare the performance of the perfect-gas ramjet to that of a ramjet utilizing a chemically reacting propellant, the diffuser operating conditions are specified and the nondimensional thrust is computed along the various other nondimensional parameters such as the exit/inlet temperature and velocity ratios. Different values for the nondimensional thrust  $F/P_1 A_1$  are determined by independently varying each component in the nondimensional thrust equation and the downstream flow conditions are found to be such that a specified, constant thrust level is met.

#### Optimum Ramjet Operation

It will be shown in the Results section of this paper that there is a value of the nondimensional thrust  $F/P_1 A_1$  for which the instantaneous thermal efficiency  $FV_1/\dot{Q}$  is at a maximum for a specified diffuser and given free-flow inlet conditions. An approximate mathematical relationship that predicts the point of maximum efficiency for the conventional ramjet operating with a perfect-gas propellant can be derived by considering the first law of thermodynamics and the momentum equation. The quantity appearing in Eq. (5).

$$\left( \frac{P_{T7}}{P_{T1}} \frac{P_1}{P_7} \right)^{(1-\gamma)/\gamma}$$

varies by about 7% at the most, so it can be treated as a constant. By assuming that the previously mentioned quantities are constant Eq. (5) can be put into the following functional form:

$$F/\dot{m}V_1 = E(T_{T7}/T_{T1})^{1/2} - B \quad (9)$$

where  $E$  and  $B$  are constants. This equation states that the ramjet thrust varies as the square root of the heat addition rate per unit mass. Similarly, Eq. (7) can be put into the form

$$\frac{FV_1}{\dot{Q}} = \frac{C(T_{T7}/T_{T1})^{1/2} - D}{(T_{T7}/T_{T1}) - 1} \quad (10)$$

where  $C$  and  $D$  are constants.

Since the rate of heat addition per unit mass varies with  $T_{T7}/T_{T1}$ , Eq. (10) illustrates that the thrust, which varies as the square root of the rate of heat addition per unit mass [Eq. (9)], divided by the rate of heat addition per unit mass will pass through an optimum. This ratio is the instantaneous efficiency and the optimum corresponds to a ramjet characterized by a specified geometry and inlet conditions operating at maximum efficiency. The values for the constants  $C$  and  $D$  are given by

$$C = K_2(K_1 + K_3 K_4) \quad \text{and} \quad D = K_2(1 + K_3)$$

where

$$K_1 = \left\{ \frac{2}{M_1^2(\gamma-1)} \left[ 1 - \left( \frac{P_{T7}}{P_{T1}} \frac{P_1}{P_7} \right)^{(1-\gamma)/\gamma} \right] + 1 \right\}^{1/2}$$

$$K_2 = \frac{(\gamma-1)M_1^2}{1 + [(\gamma-1)/2]M_1^2}$$

$$K_3 = 1/M_1^2 \gamma$$

$$K_4 = \frac{[(P_{T7}/P_{T1})(P_1/P_7)]^{(1-\gamma)/\gamma}}{K_1}$$

These relations are valid where  $P_7/P_1 = 1$  and the stagnation pressure ratio  $P_{T5}/P_{T4}$  takes on typical values in the range of 0.8-1.0. By differentiating the instantaneous efficiency [Eq. (10)] with respect to the stagnation temperature ratio, the stagnation temperature ratio giving the optimum instantaneous efficiency can be computed. The expression for this optimum ratio is

$$\left( \frac{T_{T7}}{T_{T1}} \right)_{FV_1/\dot{Q}=\max} = \left[ \frac{D}{C} + \left( \frac{D^2}{C^2} - 1 \right)^{1/2} \right]^2 \quad (11)$$

#### Results

It is instructive to examine a ramjet operating at a typical flight velocity that would be encountered at one point in a launch sequence so that the influence of the various operational parameters can be established. In order to do this, several different ramjet configurations have been analyzed for a moderate flight velocity of 7000 m/s. A diffuser cone half-angle  $\delta$  of 30 deg, a static temperature  $T_1$  of 300 K, diffuser shoulder diameter-to-tube diameter  $d_3/d_1$ , and heat addition region diameter-to-tube diameter  $d_4/d_1$  ratios of 0.805 and 0.403, respectively, have been used in the analysis. (See Fig. 1.) The 30 deg cone angle assured conical shock attachment and reasonable diffuser efficiency. The static temperature  $T_1$  was selected as a reasonable value that could exist in an actual device. The diameter ratios resulted in adequate center body structural integrity and they were also such that choking at the diffuser throat was precluded. The specific ramjet configurations examined were: 1) the conventional ramjet utilizing diatomic hydrogen that behaves as a perfect gas when it is a working fluid and with the constraint that the inlet and outlet

static pressures are equal, 2) the annular flow electrothermal ramjet operating with the same perfect gas and with the constraint that the inlet and outlet flow areas are equal, and 3) the annular flow electrothermal ramjet operating with hydrogen propellant that is allowed to dissociate and ionize and to have vibrational and electronic modes of energy storage along with finite chemical relaxation rates occurring in the supersonic nozzle expansion. For this latter case, two thrust levels per unit cross-sectional area of the tube have been specified. The higher value for the thrust per unit area is  $F/A_1 = 9.5 \times 10^7$  Pa and the lower value for the thrust per unit area is  $F/A_1 = 9.5 \times 10^6$  Pa. Two values have been considered so that the effect of varying the initial pressure in the launch tube can be illustrated for high and low values of the thrust per unit area.

Figure 2 illustrates the relationship between the instantaneous efficiency  $FV_1/\dot{Q}$  and the nondimensional thrust  $F/P_1 A_1$  for the previously mentioned operational parameters. Increasing the nondimensional thrust implies increasing the heat addition per unit mass to the propellant. The perfect-gas conventional ramjet is shown to exhibit the best performance and the optimum value for instantaneous efficiency is seen to occur at a nondimensional thrust of 12 for the conventional ramjet. This peak value is predicted to first order by Eqs. (3), (10), and (11).

The consequence of not expanding the supersonic nozzle flow to the pressure ratio  $P_7/P_1$  of unity is illustrated in Fig. 2 by the curve for the electrothermal plug ramjet operating with a perfect gas (no dissociation). Its performance is seen to be degraded substantially with respect to the conventional ramjet operating with a perfect gas. The other curves (which illustrate the effects of chemical freezing, dissociation, ionization, and vibrational and electronic modes of energy storage) are shown to exhibit performance that is similar but inferior to the electrothermal plug ramjet operating with a perfect gas. It is noted that the dissociating propellant curves of Fig. 2 were generated by fixing the thrust-to-cross-sectional area ratio  $F/A_1$  and varying the initial pressure in the launch tube  $P_1$ . The maximum value of the nondimensional thrust for which each curve shown in Fig. 2 terminates is that value for which no more heat could be added to the heat addition region of the respective ramjets without choking the flow at the exit of heat addition region 5. All of the curves in Fig. 2 illustrate that, for a given velocity and diffuser geometry, there is a value for the nondimensional thrust providing the maximum instantaneous efficiency. It is also evident that, for the case of a dissociating propellant, a high-tube-pressure/high-thrust device corresponding to the higher thrust per unit area ( $F/A_1 = 9.5 \times 10^7$  Pa) provides performance superior to a low-tube-pressure/low-thrust device ( $F/A_1 = 9.5 \times 10^6$  Pa). This is due to the greater level of dissociation occurring at the lower pressures. Figure 3 illustrates this by showing that the mass fraction of diatomic hydrogen in the ramjet exhaust is greater at the level of higher thrust per unit area where the initial tube pressure is higher at a given nondimensional thrust. It is evident that high values of the nondimensional thrust can be achieved before dissociation becomes important and that increasing the initial tube pressure  $P_1$  decreases the amount of dissociation in the propellant.

Figure 4 shows the effect of nondimensional thrust on the fraction of the total thrust produced by the differential pressure/area product across the ramjet. The conventional ramjet operating with a perfect gas derives a smaller fraction of thrust from the pressure/area differential than the other ramjet configurations. The electrothermal plug ramjet operating with a perfect gas obtains a greater fraction of thrust from the differential of the pressure/area product than the conventional ramjet for a given value of the nondimensional thrust. The electrothermal ramjet analyses of the nonperfect-gas effects show that including these effects causes the pressure-induced thrust fraction to rise over that given for the perfect-gas, electrothermal ramjet. The high-tube-

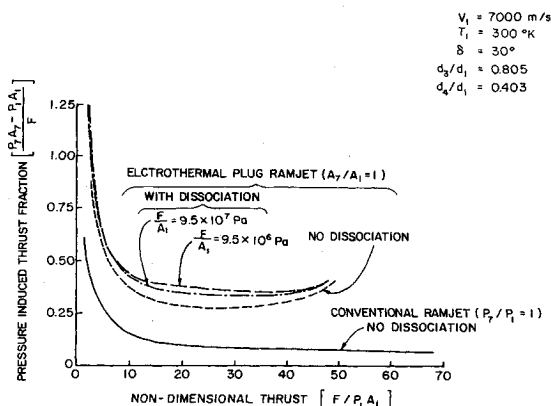


Fig. 4 Pressure-induced thrust fraction profiles.

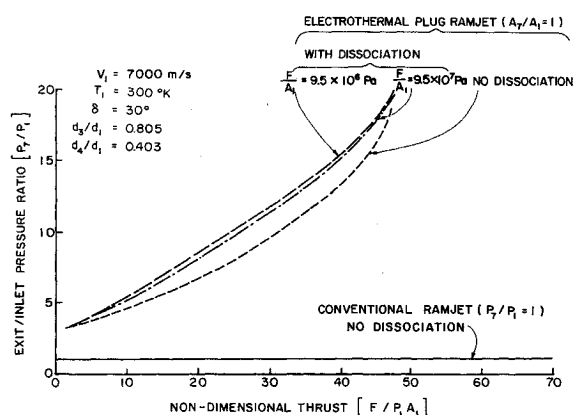


Fig. 5 Outlet/inlet pressure ratio profiles.

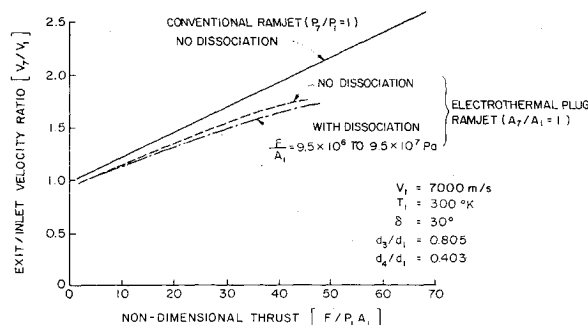


Fig. 6 Outlet/inlet velocity ratio profiles.

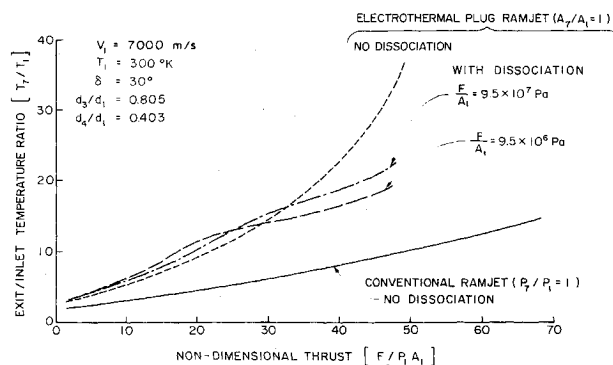


Fig. 7 Outlet/inlet static temperature ratio profiles.

pressure/high-thrust ramjet operates with a lower pressure-induced thrust fraction than the low-tube-pressure/low-thrust ramjet.

Figure 5 illustrates the relationship between the exit/inlet static pressure ratio and the nondimensional thrust for the different ramjet models considered. By design, the exit/inlet pressure ratio is unity for the conventional ramjet. The electrothermal plug ramjet operating with a perfect gas exhibits lower pressure ratios than the electrothermal plug ramjet operating with a reacting propellant. For the electrothermal plug ramjet operating with a reacting propellant, high-thrust/high-pressure operation is seen to exhibit slightly lower exit/inlet pressure ratios than low-thrust/low-pressure operation.

The exit/inlet velocity ratios for the different ramjet configurations are shown in Fig. 6. The conventional ramjet exhibits a nearly linear dependence between the exit/inlet velocity ratio and the nondimensional thrust. It has been suggested previously that, for a conventional ramjet, both the thrust [Eq. (9)] and the exit/inlet velocity ratio [Eq. (8)] show rates of change approximately proportional to the square root of the total temperature ratio  $T_7/T_1$ , so that a linear dependency between the thrust and the exit/inlet velocity ratio is to

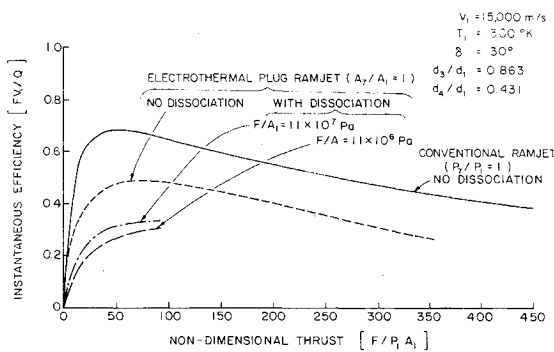


Fig. 8 Instantaneous efficiency profiles at high velocity.

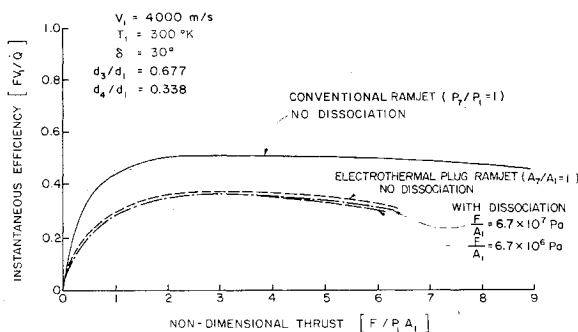


Fig. 9 Instantaneous efficiency profiles at low velocity.

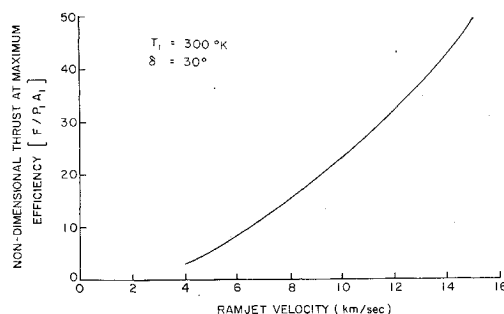


Fig. 10 Nondimensional thrust profile for maximum efficiency.

be expected. The results obtained for the electrothermal plug ramjet operating with a perfect gas show that the velocity ratio is degraded with respect to the conventional ramjet. This curve is not linear because the outlet/inlet static pressure ratio increases with nondimensional thrust for the plug ramjet [a nearly constant static pressure ratio is essential to insure linearity, as described by Eqs. (4) and (5)]. The electrothermal plug ramjet results including dissociation demonstrate that the exit/inlet velocity ratio is degraded with respect to the perfect-gas configurations. Only one curve is shown for the cases including dissociation. This is because the data for the two different cases were very close and a true distinction was difficult to show graphically. The actual data indicate that the high-thrust/high-pressure device operates with a slightly greater velocity ratio than the low-thrust/low-pressure device. This degradation in the momentum change of the propellant between the inlet and outlet is offset by greater exit/inlet pressure ratios so that desired thrust levels can be achieved.

Figure 6 also brings to light the fact that the exit/inlet velocity ratio can be less than unity. This implies a momentum change of the propellant detracts from the thrust and requires that the differential pressure/area product must supply more thrust. In Fig. 4, these regions of operation where the pressure-induced thrust fraction is greater than unity are observed at the low normalized thrusts where the velocity ratio  $V_7/V_1$  is less than unity. These regions also correspond to the low-efficiency regions illustrated in Fig. 2.

In Fig. 7 the relationship between the exit/inlet temperature ratio and the nondimensional thrust is illustrated for the different ramjet configurations. The conventional ramjet exhibits a lower temperature ratio than the other ramjet configurations because of the more complete nozzle expansion. In the case of the electrothermal plug ramjet, the dissociating propellant cases are shown initially to exhibit greater temperature ratios than the electrothermal plug ramjet operating with a perfect gas and the temperature ratios for the dissociating propellant drop below those shown for the perfect-gas electrothermal plug ramjet as the nondimensional thrust is increased. This lowering of the exit/inlet temperature ratio is due to the dissociation of the propellant.

The effect of changes in the flight velocity on the instantaneous efficiency can be seen by comparing the results of Fig. 2 ( $V_1 = 7000$  m/s) with those of Fig. 8 ( $V_1 = 15,000$  m/s) and Fig. 9 ( $V_1 = 4000$  m/s). All of the other operational parameters mentioned previously, such as the diffuser cone half-angle, are the same as for the 7000 m/s flight velocity, except for the diameter ratios  $d_3/d_1$  and  $d_4/d_1$ . The diameter ratio  $d_3/d_1 = 2$  has been specified to be constant for any velocity. As the ramjet flight velocity increases, the conical shock angle will decrease if the conical diffuser half-angle is held constant. Because it has previously been specified that the intersection of the oblique shock and the tube wall occurs at the diffuser shoulder, the tube diameter must decrease as the projectile velocity increases for a constant ramjet annular diffuser geometry. This is why the diameter ratios  $d_3/d_1$  and  $d_4/d_1$  increase as the flight velocity increases. Examining Figs. 8 and 9,

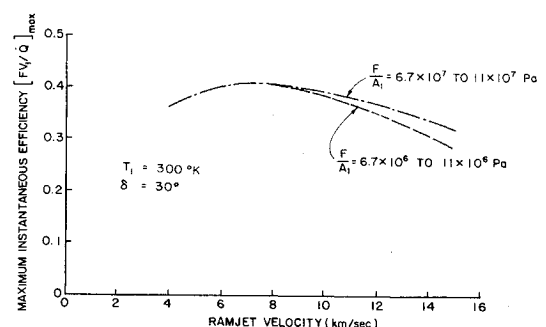


Fig. 11 Maximum instantaneous efficiency profiles.

one sees that the same trends associated with the 7000 m/s results are evident in these figures (i.e., there is a value of the nondimensional thrust for which the instantaneous efficiency is optimized). A very important feature of ramjet operation is brought out by examining Figs. 2, 8, and 9. This feature is that in order for ramjet operation to remain at a reasonable efficiency level during acceleration, the nondimensional thrust must vary greatly over the region of acceleration. Assuming that a constant thrust level  $F$  is desired and that the inlet area  $A_1$  does not change appreciably during the launch of a given plug projectile makes it apparent that the static propellant pressure immediately upstream of the ramjet must decrease as the ramjet velocity increases, so that efficient operation can be maintained. It is noted that the data in Fig. 8 for the dissociating propellant, electrothermal plug ramjet are terminated at a value of 90 for the nondimensional thrust because ionization of the propellant started to become significant past this value.

The results of Fig. 10 were obtained from a series of plots like those in Figs. 2, 8, and 9. They illustrate the variation in the nondimensional thrust that must be achieved to attain the maximum instantaneous efficiency over a velocity range of 4000-15,000 m/s. The nondimensional thrust is observed to vary from a minimum of 4 at 4000 m/s to a maximum of around 50 for a velocity of 15,000 m/s. These results are for the dissociating propellant.

Figure 11 illustrates the maximum instantaneous efficiency attainable for a mission where a projectile is accelerated from 4000 to 15,000 m/s utilizing two different thrust levels. The operational parameters are the same as previously defined. To attain the performance shown in Fig. 11, the nondimensional thrust must follow the nondimensionalized thrust profile given in Fig. 10. This means that  $P_1$  must be varied continuously along the launch tube. For high velocities, the high-thrust profile exhibits performance superior to the low-thrust profile because high static tube pressures are associated with high-thrust operation and propellant dissociation is less significant for the high-pressure case than for the low-pressure one. The optimum value for the instantaneous efficiency is observed to be near 7000 m/s, because this is the velocity for which this particular diffuser performs the best. Changing the diffuser geometry will change the location of the optimum point.

Several profiles are shown in Fig. 12 detailing the performance of a ramjet as it accelerates 10 kg at a level of 30,000 g. These profiles were computed for various conical diffuser half-angles and for tube static pressures that remain at fixed values along the tube length. For purposes of comparison, the optimum efficiency performance data for the high thrust per

unit area values given earlier are plotted with the results obtained for constant-pressure tube acceleration. These values of the thrust per unit area, coupled with the specified projectile mass, produces an acceleration of 30,000 g. The early portions of the curves where no data are shown are those portions of the launches where the ramjet propulsion system could not achieve the specified thrust and where acceleration induced by a light gas gun would be used. The influence of the tube pressure can be clearly seen by comparing the results for tube pressures  $P_1$  of 30 and 60 atm and for a conical half-angle of 30 deg. Early in the operation, a high tube pressure is shown to exhibit superior performance, while toward the end of the acceleration period the lower tube pressure exhibits the superior performance. The results plotted for the optimum performance suggest that the variation in tube pressure is important in order to maintain high efficiency.

The effect of varying the conical diffuser half-angle is also illustrated in Fig. 12. Having a diffuser cone half-angle that is either too shallow or too steep degrades the performance. For the missions analyzed in this paper, the overall optimum conical half-angle was near 30 deg.

By applying the first law of thermodynamics and the momentum equation to the control volume shown in Fig. 1b, expressions for the nondimensional thrust and the instantaneous efficiency can be put in the following forms, respectively:

$$\frac{F}{P_1 A_1} = \frac{\rho_1 V_1^2 (V_7/V_1 - 1) + P_1 (P_7/P_1 - 1)}{P_1} \quad (12)$$

$$\frac{FV_1}{\dot{Q}} = \frac{\rho_1 V_1^2 (V_7/V_1 - 1) + P_1 (P_7/P_1 - 1)}{\rho_1 q} \quad (13)$$

Examination of Eqs. (12) and (13) illustrates that, for given constant inlet conditions, the nondimensional thrust and the instantaneous efficiency will remain constant if the heat addition per unit mass  $q$ , the exit/inlet velocity ratio  $V_7/V_1$ , and the exit/inlet pressure ratio  $P_7/P_1$  remain constant. In order for these parameters to remain constant, it is required that the propellant thermodynamic properties remain constant throughout the ramjet flowfield shown in Fig. 1b. To insure a consistent solution for the flowfield at state 4 shown in Fig. 1b, it is necessary to keep the diameter ratio  $d_4/d_1$  and the conical diffuser half-angle  $\delta$  constant for whatever flight velocity is being considered. Keeping these variables constant allows the results given there to be scaled for different size projectiles and thrust levels.

The results contained in this paper assume quasiequilibrium fluid flow. Preliminary calculations regarding the effects of the unsteady flowfields have been made<sup>5</sup> and the results of these calculations suggest that the errors incurred by assuming quasiequilibrium fluid flow are not unreasonable. These calculations are made by considering the variation in the flowfield variables during a typical fluid particle residence time. The error is on the order of 15% for a velocity of 4000 m/s and decreases to the order of 5% for a velocity of 15,000 m/s. The decrease in error is due to an increase in the projectile velocity and a corresponding decrease in the fluid particle residence time. These errors were evaluated for a projectile length of 1.25 m.

Fluid particle residence times in the supersonic nozzle expansion were compared to characteristic chemical relaxation times and it was found that the residence times were typically much larger than the chemical relaxation times, so the nozzle was usually found to be operating very close to the chemical equilibrium conditions. This situation was found to exist by comparing results obtained from a model that used finite chemical reaction rates in the nozzle to those obtained assuming chemical equilibrium existed or that the Bray sudden freezing model<sup>6</sup> applied. Because of the high pressures that exist in this device, the finite reaction rate models always yielded

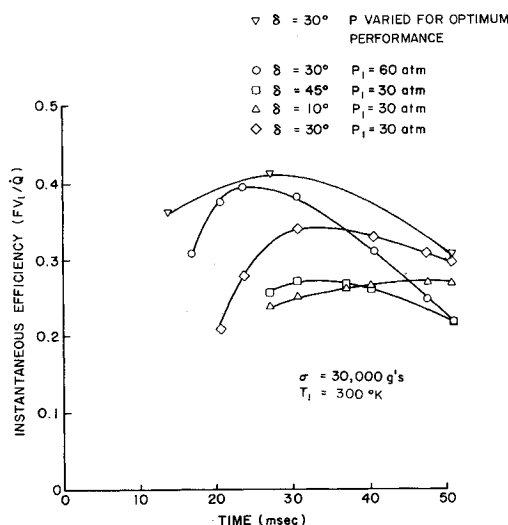


Fig. 12 Efficiency profiles over typical launch cycles.

results close to those predicted by the equilibrium model. Translational, rotational, and vibrational equilibrium of the molecules was assumed throughout the analysis. The verification of chemical equilibrium assures the validity of this assumption because chemical relaxation times are typically larger than translational, rotational, and vibrational relaxation times.

### Conclusions

It has been demonstrated that the annular flow electrothermal plug ramjet is a potentially viable high-acceleration, high-velocity launch system. Losses due to dissociation and ionization of the hydrogen propellant are typically not large. Proper diffuser design characterized by a diffuser cone half-angle near 30 deg for the case considered here minimizes diffuser shock losses so ramjet performance is not degraded to unacceptably low levels. The ramjet propellant flowfield is typically near thermodynamic equilibrium conditions. Proper tailoring of the static propellant pressure immediately upstream of the ramjet is needed to assure operation at peak efficiency over the complete ramjet velocity range that might be expected. To maintain peak efficiency, the static propellant pressure immediately ahead of the ramjet must decrease as the ramjet velocity increases. For specified ramjet operational conditions, there are values for the rate of heat addition per unit mass and the thrust per unit inlet area for which the instantaneous thermal efficiency is maximized. The assumption of

quasisteady fluid flow does not appear to invalidate the results presented in this paper.

Much analysis remains to be done to investigate completely the effects of all the parameters of concern. Additional work related to the maintenance of the correct projectile base pressure, details of the heat addition to the propellant, unsteady gas dynamics effects, and projectile material considerations remains to be done. Results contained in this paper suggest, however, that the electrothermal ramjet concept cannot be rejected on the basis that it violates a basic principle of fluid mechanics or thermodynamics. Further, the results presented suggest that the electrothermal ramjet has the potential of accelerating payloads to high velocities with good energy utilization efficiencies.

### References

- <sup>1</sup>Wilbur, P. J., Mitchell, C. E., and Shaw, B. D., "The Electrothermal Ramjet," *Journal of Spacecraft and Rockets*, Nov.-Dec. 1983, pp. 603-610.
- <sup>2</sup>Shaw, B. D., "The Electrothermal Ramjet," *Advanced Ion Thruster and Electrothermal Launcher Research*, edited by P. J. Wilbur, NASA CR-168083, Jan. 1983, pp. 36-48.
- <sup>3</sup>Lukasiewicz, J., *Experimental Methods of Hypersonics*, Marcel Dekker, Inc., 1973, pp. 95-101.
- <sup>4</sup>Anderson, J. D., *Modern Compressible Flow*, McGraw-Hill Book Co., New York, 1982, Chap. 10.
- <sup>5</sup>Shaw, B. D., "The Annular Flow Electrothermal Ramjet," edited by P. J. Wilbur, NASA CR-174704, pp. 96-104.
- <sup>6</sup>Vincenti, W. G. and Kruger, C. H., *Introduction to Physical Gas Dynamics*, John Wiley & Sons, New York, 1965, p. 298.

*From the AIAA Progress in Astronautics and Aeronautics Series . . .*

## TRANSONIC AERODYNAMICS—v. 81

*Edited by David Nixon, Nielsen Engineering & Research, Inc.*

Forty years ago in the early 1940s the advent of high-performance military aircraft that could reach transonic speeds in a dive led to a concentration of research effort, experimental and theoretical, in transonic flow. For a variety of reasons, fundamental progress was slow until the availability of large computers in the late 1960s initiated the present resurgence of interest in the topic. Since that time, prediction methods have developed rapidly and, together with the impetus given by the fuel shortage and the high cost of fuel to the evolution of energy-efficient aircraft, have led to major advances in the understanding of the physical nature of transonic flow. In spite of this growth in knowledge, no book has appeared that treats the advances of the past decade, even in the limited field of steady-state flows. A major feature of the present book is the balance in presentation between theory and numerical analyses on the one hand and the case studies of application to practical aerodynamic design problems in the aviation industry on the other.

*Published in 1982, 669 pp., 6×9, illus., \$45.00 Mem., \$75.00 List*

TO ORDER WRITE: Publications Dept., AIAA, 1633 Broadway, New York, N.Y. 10019